J. Phys. B: At. Mol. Opt. Phys. 27 (1994) 3695–3706. Printed in the UK

Electron capture and transfer ionization in collisions of H^+ and He^{2+} ions with Fe atoms

C J Patton, M A Bolorizadeh†, M B Shah, J Geddes and H B Gilbody
Department of Pure and Applied Physics The Queen's University of Belfast, Belfast, UK

Received 4 January 1994, in final form 22 March 1994

Abstract. A crossed beam technique incorporating time-of-flight spectroscopy and coincidence counting of fast ion (atom)–slow ion collision products has been used to obtain for the first time separate cross sections for simple electron capture (charge transfer) and for transfer ionization in collisions involving Fe atoms. We have studied processes involving Fe^{n+} formation in one-electron capture by 70–500 keV amu^{-1} H^+ ions for n between 1 and 4 and both one and two electron capture by 37.5–360 keV amu^{-1} He^{2+} ions for n between 1 and 6. It is shown that, for the most part, total electron capture cross sections are dominated by contributions from transfer ionization processes rather than from simple charge transfer. The energy dependence of some of the measured cross sections exhibits interesting structure and the formation of the observed multicharged Fe^{n+} ions is considered in terms of a model involving electron capture of either 4s, 3d or 3p target electrons together with electron removal through binary collisions at high velocities.

1. Introduction

Modern experimental studies of multiple ionization of atoms by ion impact have evolved from the pioneering measurements of Afrosimov *et al* (1967). These were the first measurements which employed a coincidence counting technique to identify unambiguously all the relevant collision processes leading to the formation of multiply charged ions. Subsequent experiments in a number of different laboratories using variants of this technique have provided extensive data, particularly in the use of rare gas targets bombarded with a wide variety of different projectiles (see reviews by Salzborn and Müller 1986, Cocke and Olson 1991, McGuire 1991).

For H^+ and He^{2+} impact, theoretical descriptions of multiple ionization (see review by McGuire 1991) have been focused mainly on two-electron targets such as helium. Models have included consideration of multi-step collisions, shake-off mechanisms (McGuire 1982) and the creation of inner-shell vacancies followed by rearrangement (Horsdal-Pedersen and Larsen 1979). For example, Sidorovich and Nikolaev (1983) and Sidorovich *et al* (1985) have used an independent electron model (consistent with a two-step model) to calculate cross sections for single and double ionization of helium but with limited success. The independent electron model also allows the probability of multiple ionization of electrons in a given shell to be expressed in terms of a binomial distribution of single ionization probabilities (cf McGuire and Weaver 1977). Du Bois (1987) has also shown that if the ionization probability decreases exponentially with impact parameter, the multiple ionization

† Permanent address: Department of Physics, Shahid Bahonar University, Kerman, Iran.

0953-4075/94/163695+12$19.50

cross section σ_n for the production of n electrons is given by $\sigma_n = (\sigma_1)^n$ for electrons in the same shell.

DuBois (1987) has shown that for He and Ne targets, multistep collisions are dominant in the impact energy range 80–500 keV amu^{-1}. At higher energies, the shake-off mechanism is expected to become dominant. This corresponds to single ionization followed by shake-off of further electrons due to changes in electronic screening of the nucleus. For helium, calculations by McGuire (1982) and measurements of Knudsen *et al* (1984) confirm the importance of shake-off at MeV amu^{-1} energies.

Horsdal-Pedersen and Larsen (1979) have measured charge state distributions of target ions resulting from electron capture by 40–2000 keV hydrogen ions. The observed distribution shift to higher charge states as the energy is increased and electron capture form inner shells becomes increasingly important. Inner shell vacancies created within the target lead to electron rearrangement through Auger and Coster–Kronig transitions which can result in multiple ionization. The interpretation of these measurements was based on a comparison with photoionization experiments in which inner shell vacancies were created and the resulting charge distributions observed.

In spite of their relevance to both astrophysics and to fusion energy research, processes involving multiple ionization of metallic species by ion impact have received very little attention. In recent work in this laboratory (Shah *et al* 1993) we used coincidence counting techniques to study both electron capture and multiple ionization in collisions of fast H^+ and He^{2+} ions with Mg atoms. As in previous work with rare gas targets, the measurements demonstrated the importance of transfer ionization. In addition, the measured cross sections provided evidence of significant contributions from electron capture from the inner 2s and 2p electrons in Mg.

In the present work we have adapted our previous experimental approach (Shah *et al* 1993) to study multiple ionization in collisions of 70–500 keV amu^{-1} H^+ and 35–360 keV amu^{-1} He^{2+} ions with Fe atoms. The measurements are based on a crossed beam technique incorporating time of flight spectroscopy and coincidence counting of the collision products (Shah and Gilbody 1981, 1982, 1985) which has been used successfully in this laboratory in several different variants for studies of both unstable and stable targets.

Cross sections ${}_{10}\sigma_{0n}$, for the one-electron capture processes

$$H^+ + Fe \rightarrow H + Fe^{n+} + (n-1)e \tag{1}$$

have been determined for $n = 1$ to 4 where $n = 1$ corresponds to simple charge transfer and $n > 1$ corresponds to transfer ionization. In the case of He^{2+} impact, cross sections ${}_{20}\sigma_{1n}$ for the one-electron capture processes

$$He^{2+} + Fe \rightarrow He^+ + Fe^{n+} + (n-1)e \tag{2}$$

for $n = 1$ to 6 have been determined where $n = 1$ corresponds to simple charge transfer and $n > 1$ corresponds to transfer ionization. Cross sections ${}_{20}\sigma_{0n}$ for the two-electron capture processes

$$He^{2+} + Fe \rightarrow He + Fe^{n+} + (n-2)e \tag{3}$$

for $n = 2$ to 6 have also been determined where $n = 2$ corresponds to simple charge transfer and $n > 2$ corresponds to transfer ionization. There have been no previous studies of these processes. In the present work, our measured relative cross sections ${}_{10}\sigma_{1n}$, ${}_{20}\sigma_{1n}$ and ${}_{20}\sigma_{0n}$

for particular values of n have been normalized by reference to our recently measured (Shah *et al* 1993) cross sections for multiple ionization of Fe by electron impact.

Apart from the basic interest, an improved knowledge of collision processes involving Fe in all stages of ionization is important in both an astrophysical context and in terms of controlled thermonuclear fusion energy research. In the latter case, Fe is one of the main metallic impurities in tokamak devices and data on processes relevant to heating, energy loss and plasma diagnostics are still very limited (cf Janev 1990).

2. Experimental approach

2.1. General description

The basic experimental arrangement was similar to that used in previous measurements (Shah and Gilbody 1981, 1982, Shah *et al* 1992) so that only the essential features need to be summarized here.

A well collimated primary beam of momentum and energy analysed H^+ or He^{2+} ions was arranged to intersect (at right angles) a thermal energy beam of Fe atoms in the ground state. The crossed beam region was maintained at a pressure of about 6×10^{-8} Torr. In this work, the primary He^{2+} beam was prepared by electron stripping of a He^+ beam in passage through a gas target. The oven source of Fe atoms was the same as that used in our recent studies of the electron impact ionization of Fe (Shah *et al* 1993). At the normal operating temperature of 1750°C the Fe atom beam density in the crossed beam region was estimated to be $\approx 10^{10}$ atoms cm^{-3}.

Slow Fe^{n+} collision products were extracted from the crossed beam region by a transverse electric field (applied between two high transparency grids) strong enough to ensure complete collection and counted by a particle multiplier. Fe^{n+} ions in particular charge states n could be identified and distinguished from signals due to background gas collision products by their different times of flight to the multiplier in accordance with their charge to mass ratios. As in our earlier work (cf Shah *et al* 1985), the signal S_n corresponding to the Fe^{n+} yield per unit primary ion current was recorded as the potential difference through which the ions were accelerated was increased from 3 kV to 6 kV. Again it was found that signal ratios S_n/S_1 for $n > 1$ became constant above 4.5 kV, indicating that the counting efficiency was essentially independent of n.

The primary ion beam was charge analysed by electrostatic deflection beyond the crossed beam region and a particle multiplier was used to count the selected fast H, He^+ or He products of electron capture. These selected fast particle products arising from electron capture were counted in coincidence with the slow Fe^{n+} ions of specified n arising from the same collision events. A typical fast particle–slow ion time-of-flight coincidence spectrum is shown in figure 1. The separate peaks corresponding to the formation of Fe^+, Fe^{2+}, Fe^{3+}, Fe^{4+}, Fe^{5+} and Fe^{6+} can be seen to be well resolved.

2.2. Measuring, calibration and normalization procedure

The cross section σ_n for a specific electron capture process (1), (2) or (3) leading to Fe^{n+} ions in a specified state n may be expressed as

$$\sigma_n = S(Fe^{n+})/k(Fe^{n+})k(p)\mu. \tag{4}$$

Here $S(Fe^{n+})$ is the measured fast particle–slow ion coincidence signal per unit primary beam intensity corresponding to the specific capture process; $k(Fe^{n+})$ is the detection

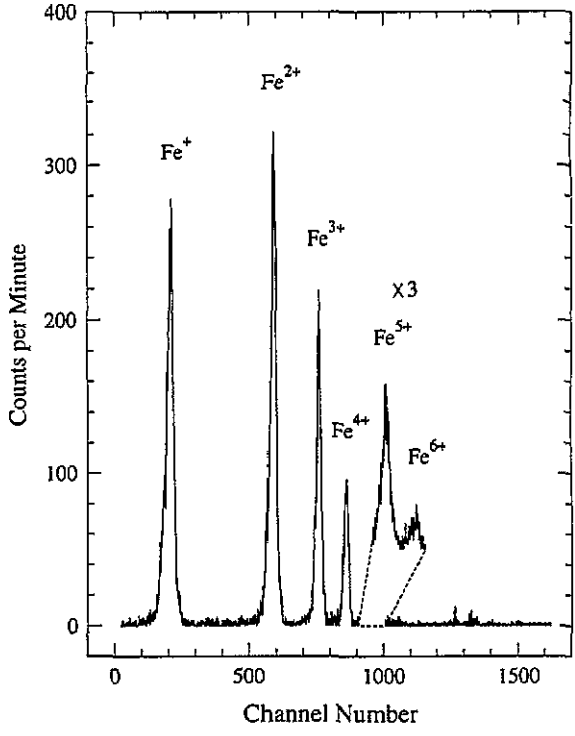

Figure 1. Fast ion/slow ion coincidence time-of-flight mass spectrum showing Fe^{n+} product yields for $n = 1$ to 6 arising from one-electron capture collisions of 46.5 keV amu^{-1} He^{2+} ions with Fe atoms. The separation between adjacent channels corresponds to a flight time difference of about 2 ns.

efficiency of the slow Fe^{n+} product ions; $k(p)$ is the detection efficiency (shown to be unity) of the fast products of electron capture formed in the primary beam; μ is the effective target thickness presented by the Fe atoms in the beam.

Our measured relative cross sections σ_n were normalized by reference to our recently measured cross sections for multiple ionization of Fe by electron impact (Shah *et al* 1993) in the manner described in our previous work (Shah *et al* 1992). By means of a sliding mount, a pulsed electron gun could be arranged to substitute an electron beam for the primary ion beam in precisely the same position with the Fe target conditions unchanged. The electron beam was pulsed with a repetition rate of 10^5 pulses s^{-1} and pulse duration of 200 ns. In this technique (Shah *et al* 1987), immediately after the transit of an electron pulse through the target beam, slow Fe^{n+} ion products formed in the crossed beam region were extracted by applying a delayed pulsed electric field across the high transparency grids.

The cross section $\sigma_n(e)$ for Fe^{n+} production by electron impact may be expressed as

$$\sigma_n(e) = S_e(Fe^{n+})/k(Fe^{n+})\mu \tag{5}$$

where $S_e(Fe^{n+})$ is the yield of Fe^{n+} ions per unit electron beam intensity. Using an electron beam energy of 200 eV and the known cross sections $\sigma_1(e)$ and $\sigma_2(e)$ given by Shah *et al* (1993), we obtained values of $k(Fe^{n+})\mu$ in (5) for $n = 1$ and 2. In a separate measurement we showed that the product $k(Fe^{n+})\mu$ for $n = 2$ to 6 was independent of n to within our measuring accuracy of 6%. These values could then be used to obtain values of σ_n in equation (4) and hence for specific electron capture processes.

Table 1. Cross sections ${}_{10}\sigma_{01}$, ${}_{10}\sigma_{02}$, ${}_{10}\sigma_{03}$, ${}_{10}\sigma_{04}$ and σ_{10} for electron capture from Fe atoms by H^+ impact.

Energy (keV amu^{-1})	${}_{10}\sigma_{01}$ (10^{-16} cm^2)	${}_{10}\sigma_{02}$ (10^{-16} cm^2)	${}_{10}\sigma_{03}$ (10^{-16} cm^2)	${}_{10}\sigma_{04}$ (10^{-16} cm^2)	σ_{10} (10^{-16} cm^2)
70	0.82 ± 0.09	0.413 ± 0.034	0.101 ± 0.023	0.0213 ± 0.0060	1.36 ± 0.10
80	0.64 ± 0.07	0.340 ± 0.024	0.092 ± 0.021	0.0199 ± 0.0060	1.09 ± 0.08
93	0.54 ± 0.06	0.292 ± 0.02	0.092 ± 0.021	0.0222 ± 0.0060	0.95 ± 0.07
108	0.42 ± 0.05	0.242 ± 0.018	0.079 ± 0.018	0.0159 ± 0.0050	0.76 ± 0.06
125	0.32 ± 0.04	0.189 ± 0.014	0.062 ± 0.014	0.0184 ± 0.0046	0.59 ± 0.04
150	0.22 ± 0.02	0.145 ± 0.012	0.058 ± 0.013	0.0141 ± 0.0033	0.44 ± 0.03
180	0.15 ± 0.016	0.110 ± 0.01	0.049 ± 0.011	0.0134 ± 0.0030	0.32 ± 0.02
210	0.11 ± 0.013	0.091 ± 0.008	0.040 ± 0.009	0.0097 ± 0.0026	0.25 ± 0.02
250	0.077 ± 0.009	0.068 ± 0.006	0.030 ± 0.007	0.0072 ± 0.0023	0.18 ± 0.01
300	0.050 ± 0.006	0.047 ± 0.008	0.022 ± 0.005	0.0062 ± 0.0010	0.13 ± 0.01
355	0.031 ± 0.004	0.034 ± 0.003	0.016 ± 0.004	0.0041 ± 0.0010	0.085 ± 0.01
420	0.021 ± 0.002	0.020 ± 0.001	0.008 ± 0.002	0.0018 ± 0.0008	0.051 ± 0.03
500	0.011 ± 0.001	0.013 ± 0.002	0.006 ± 0.002	0.0015 ± 0.0005	0.032 ± 0.03

As in our previous measurements, it was important to have a reliable continuous indication of the intensity of the Fe beam. In order to do this, a pulsed electron beam from a simple electron gun operating at 22 eV was arranged to intercept the Fe atom beam at a point beyond the main crossed beam region. The Fe^+ product ions were identified by time-of-flight spectroscopy and recorded by a channeltron. This signal was used to monitor any changes in the Fe atom beam flux.

3. Results and discussion

Tables 1–3 list our measured cross sections ${}_{10}\sigma_{0n}$ for one-electron capture by H^+ and ${}_{20}\sigma_{1n}$ and ${}_{20}\sigma_{0n}$ for both one- and two-electron capture by He^{2+} ions for n ranging from 1 to 6. In addition total electron capture cross sections $\sigma_{10} = \sum_{n=1}^{n=4} {}_{10}\sigma_{0n}$, $\sigma_{21} \simeq \sum_{n=1}^{n=6} {}_{20}\sigma_{1n}$ and $\sigma_{20} \simeq \sum_{n=2}^{n=6} {}_{20}\sigma_{0n}$ are also included. The uncertainties indicated for individual cross sections reflect 67% confidence levels based on the degree of reproducibility of the measured values. In addition, all cross sections are subject to uncertainties in absolute value arising from our normalization procedure estimated to be 12%.

Figure 2 shows our measured cross sections for ${}_{10}\sigma_{0n}$ for one-electron capture by protons in Fe together with the total cross section $\sigma_{10} \simeq \sum_{n=1}^{n=4} {}_{10}\sigma_{0n}$. While simple one-electron capture (corresponding to ${}_{10}\sigma_{01}$) makes the main contribution to σ_{10} at our lowest energy of 70 keV amu^{-1}, the transfer double ionization cross section ${}_{10}\sigma_{02}$ can be seen to exceed ${}_{10}\sigma_{01}$ at the higher energies considered. The dominant role of transfer ionization at the higher energies is illustrated by the fall in the ratio ${}_{10}\sigma_{01}/\sigma_{10}$ from 0.60 at 70 keV amu^{-1} to 0.34 at 500 keV amu^{-1}.

Figure 3 shows our measured cross sections ${}_{20}\sigma_{1n}$ for one-electron capture by He^{2+} ions in Fe together with the total cross sections $\sigma_{21} \simeq \sum_{n=1}^{n=6} {}_{20}\sigma_{1n}$. In this case, σ_{21} is large and still rising steeply towards a peak value at an energy below our low energy limit. The main contribution to σ_{21} can be seen to be provided by the simple one-electron capture cross section ${}_{20}\sigma_{11}$ only at energies below about 50 keV amu^{-1}. At higher energies the transfer ionization contributions ${}_{20}\sigma_{12}$, ${}_{20}\sigma_{13}$ and ${}_{20}\sigma_{14}$ all begin to exceed ${}_{20}\sigma_{11}$ at energies which increase with n. An indication of the importance of transfer ionization is provided

Table 2. Cross sections ${}_{20}\sigma_{11}$, ${}_{20}\sigma_{12}$, ${}_{20}\sigma_{13}$, ${}_{20}\sigma_{14}$, ${}_{20}\sigma_{15}$, ${}_{20}\sigma_{16}$ and σ_{21} for electron capture from Fe atoms by He^{2+} impact.

Energy (keV amu^{-1})	${}_{20}\sigma_{11}$ (10^{-16} cm^2)	${}_{20}\sigma_{12}$ (10^{-16} cm^2)	${}_{20}\sigma_{13}$ (10^{-16} cm^2)	${}_{20}\sigma_{14}$ (10^{-16} cm^2)
37.5	9.36 ± 0.95	5.76 ± 0.69	2.32 ± 0.17	0.89 ± 0.10
42.5	5.19 ± 0.66	3.96 ± 0.48	1.82 ± 0.15	0.76 ± 0.08
46.5	3.11 ± 0.41	2.85 ± 0.36	1.50 ± 0.14	0.59 ± 0.09
54	2.03 ± 0.27	2.41 ± 0.25	1.45 ± 0.14	0.69 ± 0.10
62.5	1.14 ± 0.17	1.86 ± 0.19	1.18 ± 0.12	0.57 ± 0.08
75	0.86 ± 0.13	1.67 ± 0.22	1.17 ± 0.13	0.61 ± 0.09
87.5	0.71 ± 0.11	1.50 ± 0.18	1.12 ± 0.11	0.62 ± 0.09
105	0.59 ± 0.09	1.26 ± 0.16	1.02 ± 0.10	0.61 ± 0.09
125	0.48 ± 0.07	0.99 ± 0.14	0.89 ± 0.09	0.58 ± 0.08
150	0.33 ± 0.06	0.78 ± 0.08	0.70 ± 0.08	0.47 ± 0.07
180	0.27 ± 0.04	0.59 ± 0.08	0.56 ± 0.06	0.40 ± 0.06
213	0.23 ± 0.03	0.49 ± 0.07	0.50 ± 0.06	0.35 ± 0.06
250	0.18 ± 0.03	0.37 ± 0.05	0.40 ± 0.05	0.29 ± 0.05
300	0.14 ± 0.03	0.29 ± 0.05	0.28 ± 0.03	0.20 ± 0.04
360	0.09 ± 0.03	0.19 ± 0.03	0.20 ± 0.02	0.14 ± 0.03

Energy (keV amu^{-1})	${}_{20}\sigma_{15}$ (10^{-16} cm^2)	${}_{20}\sigma_{16}$ (10^{-16} cm^2)	σ_{21} (10^{-16} cm^2)
37.5	—	—	18.34 ± 1.19
42.5	0.12 ± 0.03	—	11.86 ± 0.84
46.5	0.15 ± 0.03	0.023 ± 0.004	8.21 ± 0.57
54	0.19 ± 0.03	0.033 ± 0.006	6.80 ± 0.41
62.5	0.19 ± 0.03	0.038 ± 0.007	4.98 ± 0.29
75	0.22 ± 0.03	0.053 ± 0.009	4.59 ± 0.30
87.5	0.27 ± 0.03	0.053 ± 0.009	4.28 ± 0.25
105	0.26 ± 0.03	0.061 ± 0.010	3.80 ± 0.23
125	0.25 ± 0.03	0.058 ± 0.010	3.24 ± 0.20
150	0.20 ± 0.03	0.050 ± 0.008	2.53 ± 0.14
180	0.17 ± 0.03	0.038 ± 0.007	2.04 ± 0.12
213	0.14 ± 0.02	0.029 ± 0.005	1.74 ± 0.11
250	0.11 ± 0.02	0.020 ± 0.003	1.37 ± 0.09
300	0.073 ± 0.012	0.018 ± 0.003	1.01 ± 0.08
360	0.048 ± 0.009	0.010 ± 0.002	0.68 ± 0.06

by the ratio ${}_{20}\sigma_{11}/\sigma_{21}$ which decreases from 0.51 at 37.5 keV amu^{-1} to only 0.13 at 360 keV amu^{-1}.

The one-electron capture cross sections for H^+ and He^{2+} impact in figures 2 and 3 exhibit significant differences. For H^+ impact, cross sections ${}_{10}\sigma_{0n}$ for $n > 4$ were too small to measure while both ${}_{20}\sigma_{15}$ and ${}_{20}\sigma_{16}$ for He^{2+} are significant. In the latter case cross sections for $n > 6$ were too small to measure. Within the limits of uncertainty of the measurements, cross sections ${}_{10}\sigma_{0n}$ for H^+ impact fall monotonically with increasing energy for all values of n. Whereas both ${}_{10}\sigma_{01}$ and ${}_{10}\sigma_{02}$ are both approaching peak values at energies below our 70 keV amu^{-1} low energy limit, ${}_{10}\sigma_{03}$ and ${}_{10}\sigma_{04}$ appear to be peaking at energies near this limit. In the case of He^{2+} impact, σ_{21} exhibits pronounced structure with a significant 'bulge' in the curve above about 60 keV amu^{-1}. Cross sections ${}_{20}\sigma_{11}$, ${}_{20}\sigma_{12}$, ${}_{20}\sigma_{13}$ and ${}_{20}\sigma_{14}$ can be seen to be approaching peak values at energies below our low energy limit and all exhibit a 'bulge' within the present energy range which becomes more pronounced with increasing n. In each case the 'bulge' is consistent with a high energy contribution to the cross section peaking at a common energy of about 100 keV amu^{-1}. In

Table 3. Cross sections ${}_{20}\sigma_{02}$, ${}_{20}\sigma_{03}$, ${}_{20}\sigma_{04}$, ${}_{20}\sigma_{05}$, ${}_{20}\sigma_{06}$ and σ_{20} for double electron capture from Fe atoms by He^{2+} impact.

Energy (keV amu^{-1})	${}_{20}\sigma_{02}$ (10^{-16} cm^2)	${}_{20}\sigma_{03}$ (10^{-16} cm^2)	${}_{20}\sigma_{04}$ (10^{-16} cm^2)
37.5	0.26 ± 0.05	0.60 ± 0.05	0.44 ± 0.05
42.5	0.22 ± 0.05	0.50 ± 0.04	0.40 ± 0.04
46.5	0.19 ± 0.05	0.59 ± 0.04	0.50 ± 0.05
54	0.14 ± 0.02	0.45 ± 0.03	0.47 ± 0.04
62.5	0.094 ± 0.01	0.34 ± 0.03	0.36 ± 0.03
75	0.068 ± 0.008	0.25 ± 0.02	0.29 ± 0.03
87.5	0.055 ± 0.008	0.21 ± 0.02	0.26 ± 0.02
105	0.045 ± 0.007	0.15 ± 0.02	0.20 ± 0.02
125	0.032 ± 0.005	0.12 ± 0.02	0.146 ± 0.014
150	0.016 ± 0.003	0.071 ± 0.018	0.103 ± 0.010
180	0.009 ± 0.020	0.048 ± 0.021	0.064 ± 0.006
Energy (keV amu^{-1})	${}_{20}\sigma_{05}$ (10^{-16} cm^2)	${}_{20}\sigma_{06}$ (10^{-16} cm^2)	σ_{20} (10^{-16} cm^2)
37.5	0.11 ± 0.02	—	1.41 ± 0.09
42.5	0.07 ± 0.01	—	1.20 ± 0.08
46.5	0.15 ± 0.03	0.033 ± 0.007	1.46 ± 0.09
54	0.17 ± 0.03	0.036 ± 0.005	1.25 ± 0.06
62.5	0.14 ± 0.03	0.027 ± 0.004	0.97 ± 0.05
75	0.12 ± 0.02	0.023 ± 0.003	0.76 ± 0.04
87.5	0.11 ± 0.02	0.023 ± 0.003	0.66 ± 0.04
105	0.085 ± 0.016	0.021 ± 0.003	0.50 ± 0.03
125	0.068 ± 0.014	0.013 ± 0.003	0.38 ± 0.03
150	0.052 ± 0.011	0.010 ± 0.002	0.25 ± 0.02
180	0.033 ± 0.008	0.006 ± 0.001	0.16 ± 0.02

the case of ${}_{20}\sigma_{15}$ and ${}_{20}\sigma_{16}$, only this high energy contribution is evident with a single broad peak in the cross section curves centred around the same energy of 100 keV amu^{-1}.

These high energy contributions to σ_{21} which are associated with the formation of Fe^{n+} for n up to 6 cannot be explained on the basis of simple energy defect considerations. For example, the formation of Fe^{6+} ions requires an internal energy transfer of 292 eV. Jacobs *et al* (1980) in their Auger decay model show that ions up to Fe^{6+} can be produced following creation of a 2p vacancy and up to Fe^{7+} following creation of a 2s vacancy. However for the creation of an L subshell vacancy the projectile would have to transfer an energy of 708 eV (Henke *et al* 1982). For a He^{2+} projectile at the lowest energies we consider the maximum amount of energy which could be transferred in a binary collision with a stationary electron is about an order of magnitude too low to create an L shell vacancy. While the maximum energy transfer would be sufficient to create an M shell vacancy, this mechanism would not lead to the formation of Fe^{6+} ions. Indeed this model could not even account for the formation of Fe^{4+} ions which are observed in abundance with both H^+ and He^{2+} impact.

While it is not possible to account for the formation of Fe^{n+} ions of high n through the creation of inner shell vacancies, the required energy transfer from the projectile could take place in binary collisions with the target electrons. The 4s and 3d electrons on the Fe target can be considered to be essentially frozen during the collision time and symmetry considerations of electron positions suggest that, at most, the projectile ion trajectory would interact with one 4s and three 3d electrons.

The energy required to remove a single electron from the 4s, 3d, 3p and 3s subshells

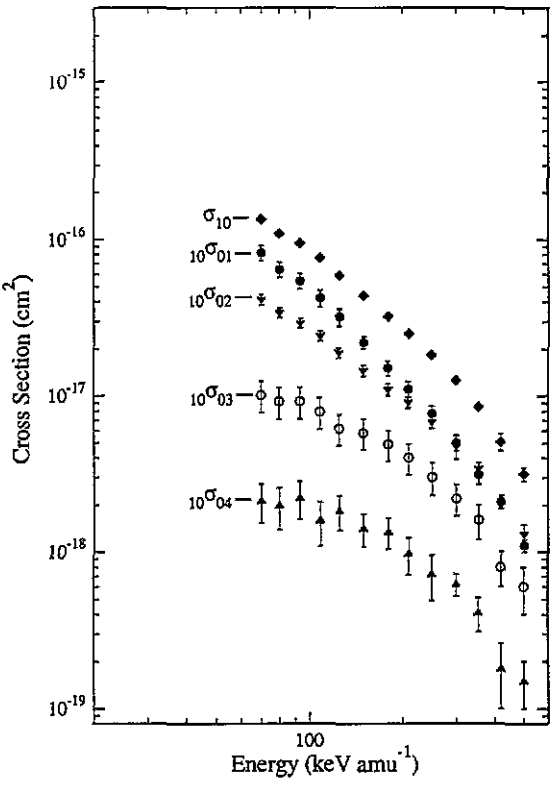

Figure 2. Cross sections $_{10}\sigma_{0n}$ for one-electron capture in collisions of H^+ with iron atoms leading to Fe^{n+} products. Total cross sections σ_{10} for one-electron capture are also shown.

is respectively 7.9 eV (Allen 1973), 13 eV, 65 eV and 93 eV (Reilman and Manson 1978). However, if more than one electron is removed at a time the actual removal energies are much higher and a rough estimate is given by

$$I = \frac{13.6(Z^* + k)^2}{n^2} \tag{6}$$

where I is the energy required to remove an electron from a given subshell of principal quantum number n when a total of k electrons have already been removed. The effective nuclear charge Z^* can be estimated from a knowledge of I for a given subshell when $k = 0$. Rough estimates obtained using (6) of the energies I required to remove the last electron from different subshells are given in table 1. At our lowest energy of about 40 keV amu^{-1} for He^{2+} impact, the maximum energy which can be transferred from the projectile to a stationary target is about 86 eV. This suggests that binary collisions can result in the ejection of only 4s or 3d electrons (but not 3p electrons) up to a total of four electrons removed.

Now let us consider the likely mechanism for transfer ionization in which electron capture is accompanied by ionization. For H^+ impact, the electron capture processes

$$H^+ + Fe \rightarrow H(1s) + Fe^+(4s^{-1}) + 5.7 \text{ eV} \tag{7}$$

$$\rightarrow H(1s) + Fe^+(3d^{-1}) + 0.6 \text{ eV} \tag{8}$$

involving capture of either a 4s or a 3d electron have small energy defects consistent with the observed rise in $_{10}\sigma_{01}$ with decreasing energy towards a peak value below our low energy

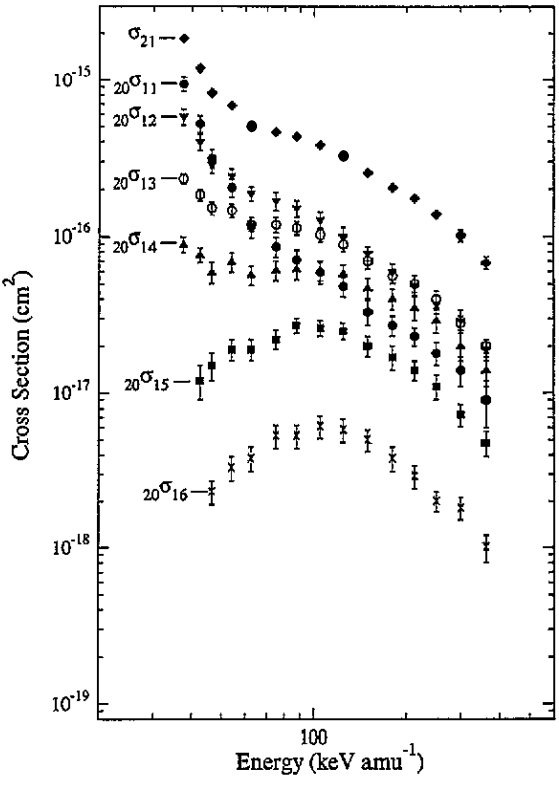

Figure 3. Cross sections $_{20}\sigma_{1n}$ for one-electron capture in collisions of He^{2+} with iron atoms leading to Fe^{n+} products. Total cross sections σ_{21} for one-electron capture are also shown.

Table 4. Energies in eV required for electron removal from Fe to produce Fe^{n+} ions.

Charge state n	1	2	3	4	5	6
Energy for removal of last electron[a]	7.9	16.2	30.6	57.1	78	102
Total energy required for removal of outermost electrons in subshells indicated	7.9 $4s^{-1}$	24.1 $4s^{-2}$	54.7 $(4s)^{-2}(3d)^{-1}$	112 $(4s)^{-2}(3d)^{-2}$	190 $(4s)^{-2}(3d)^{-3}$	292 $(4s)^{-2}(3d)^{-4}$
Estimated energy I (see text) for last electron removal in subshells indicated	7.8 $4s^{-1}$	23.3 $(4s)^{-1}(3d)^{-1}$	36.7 $(4s)^{-1}(3d)^{-2}$	53.1 $(4s)^{-1}(3d)^{-3}$	169 $(4s)^{-1}(3d)^{-3}(3p)^{-1}$	

[a] Values obtained from Allen (1973).

limit. At energies within the present range where binary encounters become important, up to four electrons can be removed from the target. We note that removal of one 4s electron and three 3d electrons would leave the target in an excited state that would decay radiatively but not by an Auger process. Our observed high energy values of $_{10}\sigma_{0n}$ for $n = 2$ to 4 reflect the probabilities of the projectile removing either one, two, three or four electrons

through binary encounters.

For one-electron capture by He^{2+} ions, it seems likely that the two exothermic processes

$$He^{2+} + Fe \rightarrow He^{+}(n = 2) + Fe^{+}(4s^{-1}) + 5.9\ eV \tag{9}$$

$$\rightarrow He^{+}(n = 2) + Fe^{+}(3d^{-1}) + 0.6\ eV \tag{10}$$

involving capture of either a 4s or 3d electron into the n = 2 state of He^{+} will be important at energies below our low energy limit at which ${}_{20}\sigma_{11}$ can be seen to be rising steeply. At energies within the present range where a 'bulge' in ${}_{20}\sigma_{12}$ is apparent, the endothermic process

$$He^{2+} + Fe \rightarrow He^{+}(1s) + Fe^{+}(3p^{-1}) - 10.6\ eV \tag{11}$$

might be expected to be important.

The observed high energy values of ${}_{20}\sigma_{1n}$ for $n = 2$ to 6 reflect the probability of electron ejection through binary collisions. Capture of a 3d electron in (10) can be accompanied by the ejection of up to three electrons (i.e. one 4s and two 3d) through binary collisions with the projectile. In the same way, 3p capture can be accompanied by the ejection of up to four electrons in binary collisions. In addition the remaining 4s electron can be ejected as a result of an Auger transition in which a 3d electron occupies the 3p vacancy. Such a mechanism would result in a total of six electrons removed in accord with our observations. The similarity in the energy dependence of the cross section curves for ${}_{20}\sigma_{15}$ and ${}_{20}\sigma_{16}$ supports this model. It is also interesting to note that, at our highest energies above 200 keV amu^{-1} the ratio ${}_{10}\sigma_{01}/{}_{10}\sigma_{02}$ for one to two electron removal by H^{+} impact and the corresponding ratio ${}_{20}\sigma_{12}/{}_{20}\sigma_{13}$ for an additional electron removed by He^{2+} impact both have a ratio of about 1.0. Similarly the ratio ${}_{10}\sigma_{02}/{}_{10}\sigma_{03}$ for two to three electron removal by H^{+} and the ratio ${}_{20}\sigma_{13}/{}_{20}\sigma_{14}$ for an additional electron removed have the not greatly different values of 0.5 and 0.7 respectively. These similar ratios for H^{+} and He^{2+} impact also suggest that the extra electron removed by He^{2+} ions arises as a result of the creation of a 3p vacancy followed by Auger decay.

Cross sections ${}_{20}\sigma_{0n}$ and $\sigma_{20} \simeq \sum_{n=2}^{n=6} {}_{20}\sigma_{0n}$ for He^{2+} impact are shown in figure 4. In this case the transfer ionization contributions ${}_{20}\sigma_{03}$ and ${}_{20}\sigma_{04}$ can be seen to provide the main contributions to the total cross section σ_{20} rather than the simple two-electron transfer term ${}_{20}\sigma_{02}$ in the energy range considered. Indeed, even the Fe^{5+} formation cross section ${}_{20}\sigma_{05}$ can be seen to exceed ${}_{20}\sigma_{02}$ at energies above about 50 keV amu^{-1}. The ratio ${}_{20}\sigma_{02}/\sigma_{20}$ decreases from 0.18 at 37.5 keV amu^{-1} to only 0.06 at 180 keV amu^{-1}. A process of the type

$$He^{2+} + Fe \rightarrow He(1s^2) + Fe^{2+}(3p^{-1} \text{ and } 4s^{-1} \text{ or } 3d^{-1}) \tag{12}$$

involving capture of a 3p electron and either a 4s or 3d electron could account for the observed values of ${}_{20}\sigma_{02}$ which increase with decreasing energy over the range considered. In addition to the two electrons captured, up to three additional electrons can be removed through binary collisions with likelihoods indicated by our observed high energy values of ${}_{20}\sigma_{03}$, ${}_{20}\sigma_{04}$ and ${}_{20}\sigma_{05}$. As in the case of ${}_{20}\sigma_{16}$ through (11), ${}_{20}\sigma_{06}$ would result from Auger decay. At high energies the similar energy dependence of the ${}_{20}\sigma_{05}$ and ${}_{20}\sigma_{06}$ cross sections is consistent with this model. It is also interesting to note that high energy ratios ${}_{20}\sigma_{04}/{}_{20}\sigma_{03}$ and ${}_{20}\sigma_{05}/{}_{20}\sigma_{04}$ have respective values of 1.3 and 0.5 which are not greatly different from the ratios ${}_{10}\sigma_{01}/{}_{10}\sigma_{02} = 1.0$ and ${}_{10}\sigma_{02}/{}_{10}\sigma_{03} = 0.45$ for H^{+} impact but with two electrons less removed. Thus compared with H^{+} ions, while He^{2+} ions remove one extra electron in the one-electron capture process, two extra electrons are removed in the two-electron capture process.

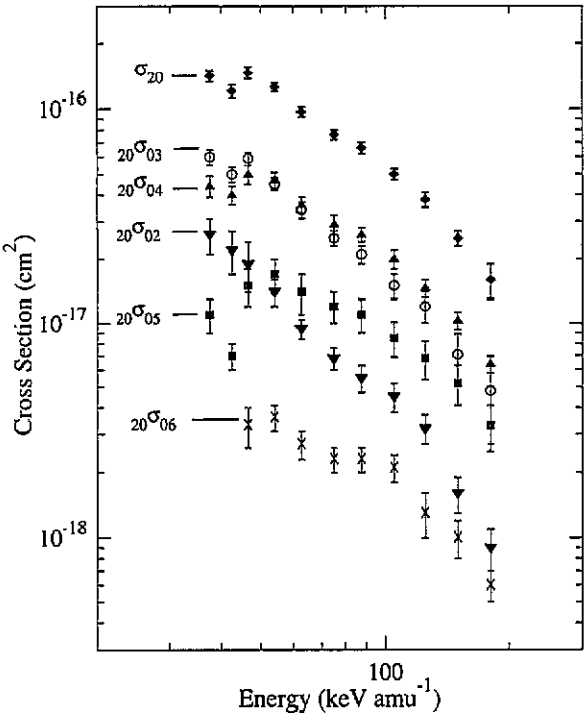

Figure 4. Cross sections $_{20}\sigma_{0n}$ for two-electron capture in collisions of He^{2+} with iron atoms leading to Fe^{n+} products. Total cross sections σ_{20} for two-electron capture are also shown.

4. Conclusions

The processes of charge transfer and transfer ionization in one-electron capture by H^+ ions and both one and two-electron capture by He^{2+} ions in collisions with Fe atoms have been studied for the first time. At the energies considered, transfer ionization processes leading to Fe^{n+} ions for up to $n = 4$ in the case of H^+ impact and up to $n = 6$ in the case of He^{2+} are shown to provide the dominant contributions to electron capture rather than simple charge transfer.

In particular, cross sections $_{20}\sigma_{1n}$ for one-electron capture by He^{2+} exhibit structure within the present energy range which cannot be explained in terms of simple energy defect considerations. A model in which electron capture of either 4s, 3d or 3p target electrons takes place together with the removal of additional electrons through binary collisions has been proposed which satisfactorily accounts in a qualitative way for our observations.

Acknowledgments

This research is part of a programme supported by a Rolling Research Grant from the Engineering and Physical Sciences Research Council. One of us (CJP) is indebted to the Department of Education, Northern Ireland for the award of a Research Studentship. One of us (MAB) has received the support of the Shahid Bahonar University, Iran which has allowed him to participate in this work.

References

Afrosimov V V, Mamaev Yu A, Panov M N, Uroshevich V and Fedorenko V 1967 *Sov. Phys.–Tech. Phys.* **12** 394

Allen C W 1973 *Astrophysical Quantities* (London: Athlone) p 36

Cocke C L and Olson R E 1991 *Phys. Rep.* **205** 152

DuBois R D 1987 *Phys. Rev.* A **36** 2585

Henke B L, Lee P, Tanaka T J, Shimabukyo R L and Fujikawa B K 1982 *At. Data Nucl Data Tables* **27** 1

Horsdal-Pedersen E and Larsen L 1979 *J. Phys. B: At. Mol. Phys.* **12** 4085

Jacobs V L, Davis J, Rozsnyyai B F and Cooper J W 1980 *Phys. Rev.* A **21** 1917

Janev R K (ed) 1990 *Atomic and Molecular Data for Metallic Impurities in Fusion Plasmas* (IAEA Report INDC (NDS) - 236/M5) (Vienna: IAEA) p 22

Knudsen H, Andersen L H, Hvelplund P, Astner G, Cederquist H, Danared H, Liljeby L and Rensfelt K-G 1984 *J. Phys. B: At. Mol. Phys.* **17** 3545

McGuire J H 1982 *Phys. Rev. Lett.* **49** 1153

—— 1991 *Adv. At. Mol. Opt. Phys.* **29** 217

McGuire J H and Weaver L 1977 *Phys. Rev.* A **16** 41

Reilman R F and Manson S T 1978 *Phys. Rev.* A **18** 2124

Salzborn E and Müller A 1986 *NATO Advanced Studies Institute Series B* **145** ed F Brouillard (New York: Plenum) pp 357

Shah M B, Elliott D S and Gilbody H B 1987 *J. Phys. B: At. Mol. Phys.* **20** 3501

Shah M B and Gilbody H B 1981 *J. Phys. B: At. Mol. Phys.* **14** 2361

—— 1982 *J. Phys. B: At. Mol. Phys.* **15** 3441

—— *1985 J. Phys. B: At. Mol. Phys.* **18** 899

Shah M B, McCallion P, Itoh Y and Gilbody H B 1992 *J. Phys. B: At. Mol. Opt. Phys.* **25** 3693

Shah M B, McCallion P, Okuno K and Gilbody H B 1993 *J. Phys. B: At. Mol. Opt. Phys.* **26** 2393

Sidorovich V A and Nikolaev V S 1983 *J. Phys. B: At. Mol. Phys.* **16** 3243

Sidorovich V A, Nikolaev V S and McGuire J H 1985 *Phys. Rev.* A **31** 2193